η^5-Semiquinone Complexes and the Related η^4-Benzoquinone of (Pentamethylcyclopentadienyl)rhodium and -iridium: Synthesis, Structures, Hydrogen Bonding, and Electrochemical Behavior

Jamal Moussa, Carine Guyard-Duhayon, Patrick Herson, and Hani Amouri*

Laboratoire de Chimie Inorganique et Matériaux Moléculaires UMR 7071-CNRS, Université Pierre et Marie Curie, 4, place Jussieu, case 42, 75252 Paris Cedex 05, France

Marie Noelle Rager

Ecole Nationale Supérieure de Chimie de Paris, 11 Rue Pierre et Marie Curie, 75231 Paris Cedex 05, France

Anny Jutand*

Ecole Normale Supérieure, Département de chimie UMR CNRS-ENS-UPMC 8640, 24 Rue Lhomond, 75231 Paris Cedex 05, France

Received September 10, 2004

Treatment of hydroquinone with $[Cp^*M(solvent)_3][OTf]_2$ (M = Rh, Ir) in acetone afforded the π-bonded complexes $\{[Cp^*M(\eta^5\text{-semiquinone})][OTf]\}_n$ (M = Rh (**1a**), M = Ir (**1b**)) in 95% yield. The ^{1}H NMR spectra of **1a**,**b** recorded in CD_3OD indicate strong hydrogen bonding in solution. The crystal structures of **1a** and **1b** were determined and exhibit strong intermolecular hydrogen bonding, forming organometallic polymers in which the integrity of the system is maintained by hydrogen bonding between metal−semiquinone subunits. Deprotonation of **1a** produced the related η^4-quinone complex $[Cp^*Rh(\eta^4\text{-quinone})]$ (**2a**), which was fully characterized and its X-ray molecular structure determined. Furthermore, the electrochemical behavior of these η^4-quinone π-complexes $[Cp^*M(\eta^4\text{-quinone})]$ (M = Rh (**2a**), M = Ir (**2b**)) was investigated and compared to that of the well-known couple quinone/hydroquinone. The latter are important species in chemistry and biology; their biological action is often linked to their electron-transfer rates and redox behavior.

Introduction

Quinones are considered a prominent class of compounds and play an important role in chemistry and biology.[1] For instance, vitamin K possesses a quinone function in its structure.[2] Their biological action is often linked to their electron-transfer rates and redox behavior.[3] Quinone/hydroquinone redox couples have been widely used in electrochemical studies because they are readily available and exhibit "well behaved" electrochemistry.[4] Surprisingly, examples of metal complexes where hydroquinone or quinone acts as a π-bonded ligand are few.[5,6] For instance, we note that Sweigart and co-workers reported[7] the synthesis of η^4-quinone complexes of manganese tricarbonyl and the related η^5-semiquinones; however, the chromium analogue $Cr(CO)_3(\eta^6\text{-hydroquinone})$ was reported to be thermally unstable and air sensitive and, hence, could not be isolated.[8] Therefore, the nature of the metal and the auxiliary ligands plays an important role in stabilizing these quinone/hydroquinone complexes. In 1998 we reported the synthesis of the first stable iridium hydroquinone complex, $[Cp^*Ir(\eta^6\text{-hydroquinone})]^{2+}$.[9] Subsequent deprotonation gave the related η^5-semiquinone and η^4-quinone compounds. The latter can be protonated to give the starting material (Schemes 1 and 2).

* To whom correspondence should be addressed. E-mail: amouri@ccr.jussieu.fr (H.A.).

(1) (a) Larsen, P. L.; Clarke, C. F. *Science* **2002**, *295*, 120. (b) Do, T. Q.; Hsu, A. Y.; Jonassen, T.; Lee, P. T.; Clarke, C. F. *J. Biol. Chem.* **2001**, *276*, 18161. (c) Steinberg-Yfrach, G.; Liddell, P. A.; Moore, A. L.; Gust, D.; Moore, T. A. *Nature* **1997**, *385*, 239. (d) Cross, J. V.; Deak, J. C.; Rich, E. A.; Qian, Y.; Lewis, M.; Parrott, L. A.; Mochida, K.; Gustfason, D.; Vande Pol, S.; Templeton, D. J. *J. Biol. Chem.* **1999**, *274*, 31150.

(2) Lamson, D. W.; Plaza, S. M. *Altern. Med. Rev.* **2003**, *8*, 303.

(3) Voet, D.; Voet, J. B.; Pratt, C. W. *Fundamentals of Biochemistry*; Wiley: New York, 1999.

(4) (a) Parker, V. *Chem. Commun.* **1969**, 716. (b) Eggins, B.; Chambers, J. Q. *Chem. Commun.* **1969**, 232.

(5) (a) Liebeskind, L. S.; Jewell, C. F., Jr. *J. Organomet. Chem.* **1985**, *285*, 305. (b) Jewell, C. F., Jr.; Liebeskind, L. S.; Williamson, M. *J. Am. Chem. Soc.* **1985**, *107*, 6715. (c) Cho, S. H.; Wirtz, K. R.; Liebeskind, L. S. *Organometallics* **1990**, *9*, 3067.

(6) Ura, Y.; Sato, Y.; Shiotsuki, M.; Suzuki, T.; Wada, K.; Kondo, T.; Mitsudo, T. *Organometallics* **2003**, *22*, 77.

(7) Oh, M.; Carpenter, G. B.; Sweigart, D. A. *Organometallics* **2002**, *21*, 1290.

(8) (a) Wright, M. E. *J. Organomet. Chem.* **1989**, *376*, 353. (b) Schumann, H.; Arif, A. M.; Richmond, T. G. *Polyhedron* **1990**, *9*, 1677.

(9) (a) Le Bras, J.; Amouri, H.; Vaissermann, J. *Organometallics* **1998**, *17*, 1116. (b) Le Bras, J.; Amouri, H.; Vaissermann, J. *J. Organomet. Chem.* **1998**, *553*, 483.

10.1021/om049292t CCC: $27.50
Publication on Web 11/16/2004

Scheme 1

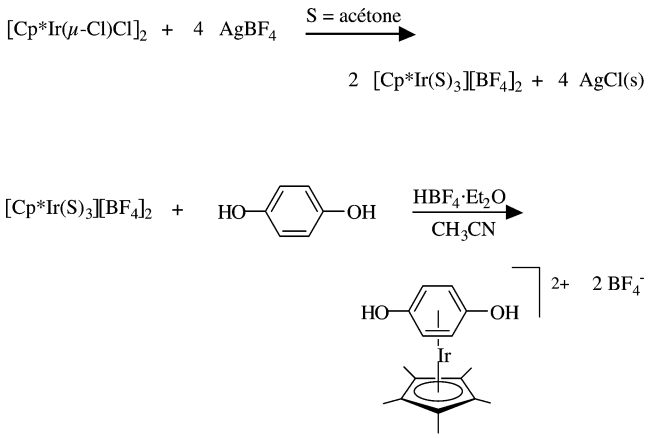

Scheme 2

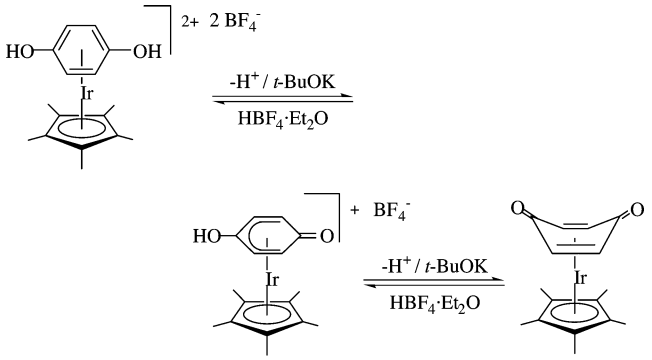

In this paper we extend our research investigations to the preparation of the related compounds of the rhodium congener not reported before. Interestingly the synthetic procedure used here differs from that described for the synthesis of [Cp*Ir(η^6-hydroquinone)]$^{2+}$. Thus, upon treatment of hydroquinone with [Cp*Rh(solvent)$_3$][CF_3SO_3]$_2$ prepared in situ in acetone[10] the compound {[Cp*Rh(η^5-semiquinone)][CF_3SO_3]}$_n$ (**1a**) was obtained and fully characterized. The related iridium complex {[Cp*Ir(η^5-semiquinone)][CF_3SO_3]}$_n$ (**1b**) was also prepared. The X-ray molecular structures of **1a**,**b** are reported and show the formation of 1D polymers, where the integrity of the system is maintained through strong hydrogen bonding. Deprotonation of **1a** provided in good yield the rhodium−quinone complex [Cp*Rh(η^4-quinone)] (**2a**). The X-ray molecular structure was determined and confirmed the formation of **2a**. The solution behavior and stability of these novel rhodium compounds are compared to those of the iridium family; furthermore, the electrochemistry of both rhodium and iridium compounds was studied and provided us with valuable information about their behavior in solution relative to the free ligand.

Results and Discussion

Preparation and X-ray Molecular Structures of the Semiquinone Complexes 1a,b. Treatment of hydroquinone with [Cp*Rh(solvent)$_3$][CF_3SO_3]$_2$ prepared in situ in acetone from the rhodium dimer [Cp*Rh(μ-Cl)Cl]$_2$ and AgOTf immediately gave a yellow solution. The latter was stirred for 15 min, and subsequent workup provided a yellow microcrystalline product in 95% yield, identified by spectroscopic data and microanalysis as {[Cp*Rh(η^5-semiquinone)][CF_3SO_3]}$_n$ (**1a**) (Scheme 3).

Scheme 3

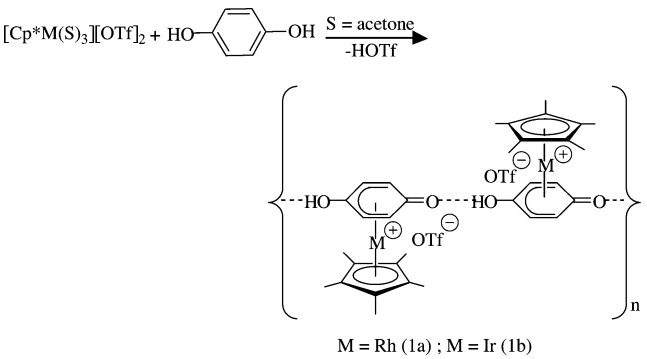

M = Rh (1a) ; M = Ir (1b)

Table 1. Crystal Data and Structure Refinement Details for 1a,b and 2a

	1a	1b	2a
formula	$C_{16}H_{20}O_2Rh\cdot CF_3SO_3$	$C_{16}H_{20}O_2Ir\cdot CF_3SO_3$	$C_{16}H_{19}O_2Rh\cdot 2H_2O$
fw	496.31	584.62	382.26
space group	$P2_1/n$	$P2_1/n$	$Pcab$
a (Å)	8.492(1)	8.5212	13.9281(8)
b (Å)	13.463(2)	13.493(1)	14.398(3)
c (Å)	33.527(5)	33.614(3)	15.554(4)
α (deg)			90
β (deg)	92.94(1)	93.464	90
γ (deg)			90
V (Å^3)	3827.9(9)	3858.0(5)	3119(1)
Z	8	8	8
ρ_{calcd} (g cm^{-3})	1.72	2.013	1.63
temp (K)	295	295	295
λ(Mo Kα) (Å)	0.710 73	0.710 73	0.710 73
μ (cm^{-1})	10.55	70.8	11.1
$R(F_o)^a$	0.0518	0.0412	0.0309
$R_w(F_o)^b$	0.0562	0.0465	0.0324

^{a} $R = [\Sigma(|F_o| - |F_c|)/\Sigma F_o$. ^{b} $R_w = [\Sigma w(|F_o| - |F_c|)^2/\Sigma w F_o^2]^{1/2}$.

The infrared spectrum recorded from KBr disks showed two strong absorptions at 1234 and 1024 cm^{-1} assigned to the triflate anion, and we also note a broad band centered at 3361 cm^{-1} attributed to −OH- - -O hydrogen bonding. The ^{1}H NMR of **1a** recorded in CD_3OD showed two singlets at δ 6.13 ppm assigned to the ring protons and at δ 2.09 ppm attributed to the methyl protons of the Cp*Rh unit. We also note the presence of a singlet at δ 6.61 ppm that by integration corresponds to 1H, which we attribute to intermolecular hydrogen bonding. In fact, upon addition of D_2O to the NMR sample tube of **1a**, a gradual disappearance of this signal was observed, indicating that indeed this signal corresponds to intermolecular hydrogen bonding.

To ascertain the structure of this novel species **1a**, crystals were grown from MeOH/ether solution. Complex **1a** crystallizes in a monoclinic unit cell, with space group $P2_1/n$. There are two independent molecules in the asymmetric unit. Refinement details are discussed in the Experimental Section. Crystallographic data for **1a** are given in Table 1. The structure (Figure 1) shows the formation of a 1D infinite chain, where simple "η^5-semiquinone−Cp*Rh" subunits are connected through

(10) (a) White, C.; Thompson, S. J.; Maitlis, P. M. *J. Chem. Soc., Dalton Trans.* **1977**, 1654. (b) White, C.; Thompson, S. J.; Maitlis, P. M. *J. Organomet. Chem.* **1977**, *127*, 415. (c) Amouri, H.; Guyard-Duhayon, C.; Vaissermann, J.; Rager, M. N. *Inorg. Chem.* **2002**, *41*, 1397.

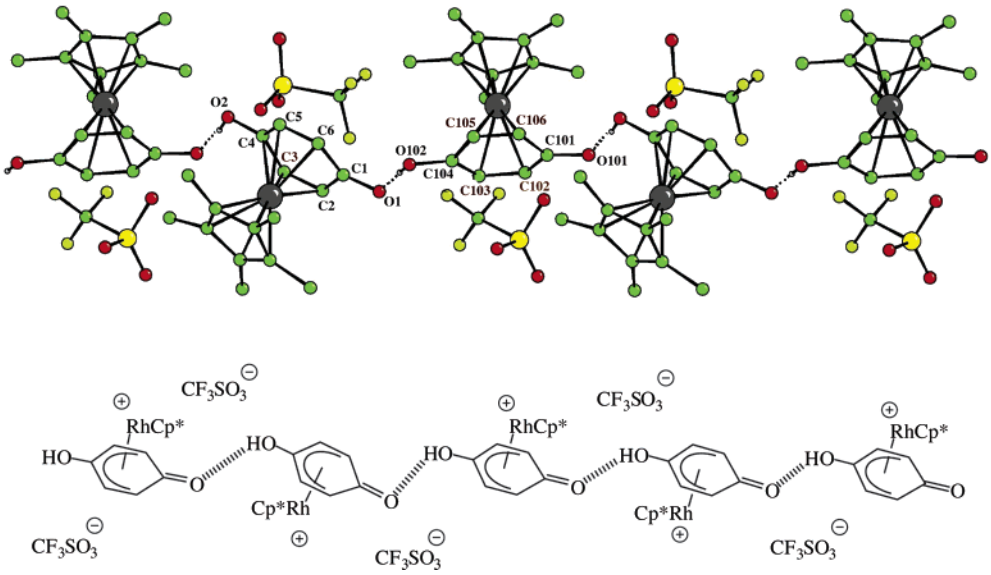

Figure 1. X-ray molecular structure of [Cp*Rh(η^5-semiquinone)] (**1a**) with the atom-numbering system. Selected bond distances (Å) and angles (deg): molecule A, Rh1−C1 = 2.349(7), Rh1−C2 = 2.218(6), Rh1−C3 = 2.219(6), Rh1−C4 = 2.318(6), Rh1−C5 = 2.221(5), Rh1−C6 = 2.219(6), C1−O1 = 1.279(9), C2−C1−C6 = 115.1(6), C3−C4−C5 = 115.7(6); molecule B, Rh2−C101 = 2.358(7), Rh2−C102 = 2.220(6), Rh2−C103 = 2.217(6), Rh2−C104 = 2.335(7), Rh2−C105 = 2.236(7), Rh2−C106 = 2.221(6), C101−O101 = 1.272(9), C102−C101−C106 = 114.7(6), C103−C104−C105 = 116.6(6).

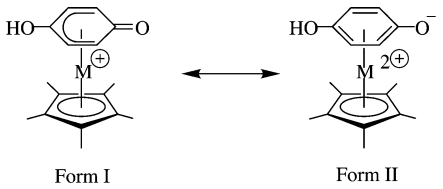

Figure 2.

strong intermolecular hydrogen bonding. This is the first Cp*M−η^5-semiquinone structure reported in the literature and the second of its type; we note that Sweigart and co-workers reported the structure of the neutral (η^5-semiquinone)Mn(CO)$_3$ complex prepared by a completely different method.[7] The hydrogen-bonded O(2)- - -O(101) distance of 2.46 Å (average) is remarkably short and can be compared to the O- - -O distance of 2.74 Å reported for the quinhydrone, where an infinite molecular chain is formed through hydrogen bonding between the hydroquinone and the quinone units.[11]

The phenolic carbon atoms of the rhodio−semiquinone unit are bent out of the diene plane by the small angles of 7.2 and 8.2°, respectively. The latter dihedral angle is less than those seen in typical [Cp*Rh(η^5-cyclohexadienyl)]$^+$ complexes.[12] This implies that the Rh1- - -C(1)/Rh2- - -C(101) and Rh1- - -C(4)/Rh2- - -C(104) bond distances (average) of 2.35 and 2.33 Å are short enough to indicate some bonding interaction at the C═O and C−OH ends of the ring. These results indicate that the coordination of the arene ring is highly symmetric, suggesting a major contribution from the η^6 resonance form II (Figure 2). Indeed, the ^{1}H and ^{13}C NMR data of **1a** support these observations; for instance, the ^{1}H NMR data show only one aromatic C−H signal and the ^{13}C NMR data show only two aromatic carbon signals. This phenomenon illustrates dynamic strong hydrogen-bonding interactions that equilibrate the −C═O and the C−OH ends of the rhodio−semiquinone subunits in polymer **1a**.

Similarly, the iridium congener {[Cp*Ir(η^5-semiquinone)][CF_3SO_3]}$_n$ (**1b**) was prepared by treating the solvated iridium species [Cp*Ir(solvent)$_3$][CF_3SO_3]$_2$, prepared in situ, with hydroquinone in acetone for 15 min (Scheme 3). The iridium 1D polymer **1b** was obtained as an off-white microcrystalline substance in 94% yield. The spectroscopic data for **1b** were close to those described for the rhodium congener {[Cp*Rh(η^5-semiquinone)][CF_3SO_3]}$_n$ (**1a**). For instance, the ^{1}H NMR of **1b** recorded in CD_3OD showed the presence of two singlets at δ 6.03 ppm, assigned to the ring protons, and at δ 2.19 ppm, attributed to the methyl protons of the Cp*Ir unit. In a way similar to that observed for **1a**, we note the presence of a singlet at δ 6.61 ppm, which integrates for 1H, that we attribute to the intermolecular hydrogen bonding. In a way similar to that observed for **1a**, addition of D_2O to an NMR sample of **1b** in CD_3OD showed a gradual disappearance of this signal. Furthermore, the infrared spectrum of **1b** also showed the presence of a large band at 3400 cm^{-1} that we attribute to intermolecular hydrogen bonding. The X-ray molecular structure of **1b** was determined. Crystallographic data for **1b** are given in Table 1. Complex **1b** crystallizes in a monoclinic unit cell, space group $P2_1/n$, which is similar to that observed for **1a**. There are two independent molecules in the asymmetric unit. Complex **1b** is isostructural with **1a**. A view of the complex and selected bond distances and angles are given in Figure 3. The structure of **1b** shows the formation of a 1D polymer where simple "η^5-semiquinone−Cp*Ir" subunits are connected through strong intermolecular hydrogen bonding.

The structure of **1b** appears to be identical with that of **1a**: for instance, the hydrogen-bonded O(2)- - -O(101) distance is, at 2.44 Å, analogous to that observed for the rhodium polymer **1a**. The phenolic carbon atoms of

(11) Sakurai, T. *Acta Crystallogr.* **1968**, *B24*, 403.
(12) (a) Le Bras, J. Amouri, H.; Vaissermann, J. *J. Organomet. Chem.* **1998**, *567*, 57 and references therein. (b) Amouri, H.; Le Bras, J. *Acc. Chem. Res.* **2002**, *35*, 501 and references therein.

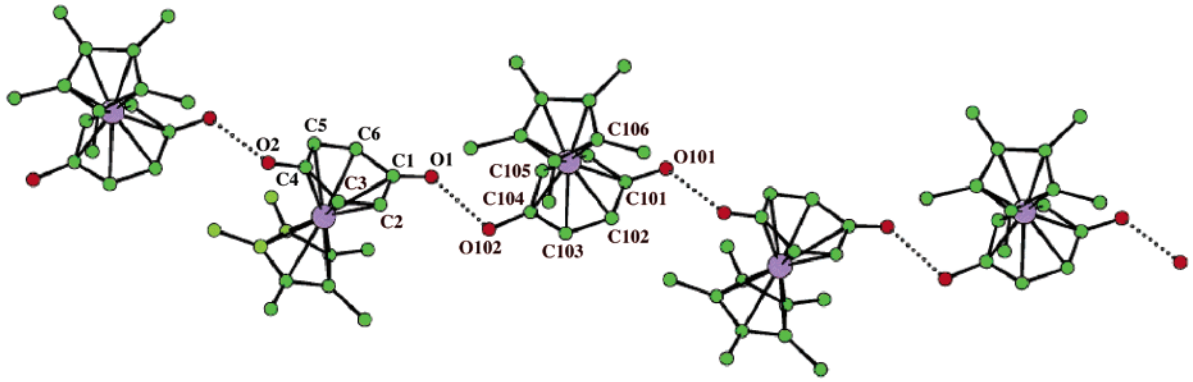

Figure 3. X-ray molecular structure of [Cp*Ir(η^5-semiquinone)] (**1b**) with the atom-numbering system. Selected bond distances (Å) and angles (deg): molecule A, Ir1−C1 = 2.339(1), Ir1−C2 = 2.210(9), Ir1−C3 = 2.213(9), Ir1−C4 = 2.396(1), Ir1−C5 = 2.228(9), Ir1−C6 = 2.232(9), C1−O1 = 1.315(1), C2−C1−C6 = 116.5(9), C3−C4−C5 = 113.9(9); molecule B, Ir2−C101 = 2.334(8), Ir2−C102 = 2.214(9), Ir2−C103 = 2.21(1), Ir2−C104 = 2.379(1), Ir2−C105 = 2.220(9), Ir2−C106 = 2.217(8), C101−O101 = 1.29(1), C102−C101−C106 = 116.5(8), C103−C104−C105 = 113.8(9).

the irido−semiquinone unit are bent out of the diene plane by small angles of 9.2 and 11.6°, respectively. These values are slightly higher than those observed for the rhodio−semiquinone species (θ = 7.2 and 8.2°) but are much smaller than those seen in typical [Cp*Ir(η^5-cyclohexadienyl)]$^+$ complexes.[12] This implies that the Ir- - -C(1) and Ir- - -C(4) bond distances of 2.34(1) and 2.396(9) Å are short enough to indicate some bonding interaction at the C=O and C−OH ends of the ring. All of these results suggest that the coordination of the arene ring in **1b** is highly symmetric and isostructural with that observed for complex **1a** (Figure 2).

Preparation and X-ray Molecular Structure of the *p*-Benzoquinone Rhodium Complex (2a). In 1998 we reported the synthesis of the X-ray molecular structure of the iridium benzoquinone complex [Cp*Ir(η^4-benzoquinone)] (**2b**) by double deprotonation of [Cp*Ir(η^6-hydroquinone)][BF_4]$_2$.[9] Since the related rhodium hydroquinone complex was not stable and could not be isolated, we sought other methods to prepare the rhodium benzoquinone complex [Cp*Rh(η^4-benzoquinone)] (**2a**). In this context we have found that the rhodium and iridium polymers {[Cp*M(η^5-semiquinone)][CF_3SO_3]}$_n$ (M = Rh (**1a**), M = Ir (**1b**)) are good precursors for the preparation of the related metal benzoquinone complexes [Cp*M(η^4-benzoquinone)] (M = Rh (**2a**), M = Ir (**2b**)). Thus, treatment of **1a** with 3 equiv of t-BuOK in CH_2Cl_2 for 3 h produced a yellow solution. Reaction workup furnished the benzoquinone rhodium complex in 60% yield as a yellow microcrystalline material. The ^{1}H and ^{13}C NMR data recorded for **2a** in CD_3CN are consistent with the proposed formula: for instance, two singlets are visible at δ 1.92 and 4.82 ppm and are assigned to the methyl protons of the "Cp*Rh" moiety and to the diene protons of the π-bonded η^4-benzoquinone. The structure of [Cp*Rh(η^4-benzoquinone)] (**2a**) was confirmed by a single-crystal X-ray diffraction study. Complex **2a** crystallizes in an orthorhombic unit cell, with space group *Pcab*. Crystallographic data for **2a** are given in Table 1. A view of the complex and selected bond distances and angles are shown in Figure 4.

As expected, the Cp*Rh moiety is coordinated to only four carbons of the π-quinone ligand, whereby the distance from the metal to the centers of the π-bonded carbons is 1.70 Å for the quinone and 1.80 Å for η^5-Cp*.

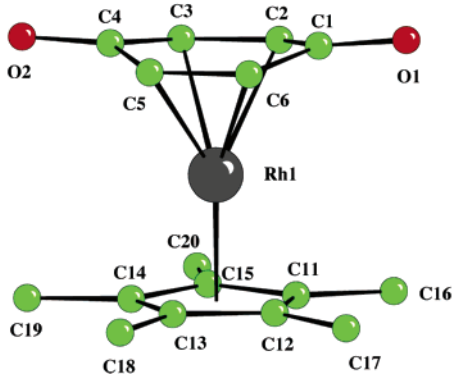

Figure 4. X-ray molecular structure of [Cp*Rh(η^4-benzoquinone)] (**2a**) with the atom-numbering system. Selected bond distances (Å) and angles (deg): Rh1−C1 = 2.403(4), Rh1−C2 = 2.207(4), Rh1−C3 = 2.195(4), Rh1−C4 = 2.366-(4), Rh1−C5 = 2.187(4), Rh1−C6 = 2.202(4), C1−O1 = 1.251(5), C4−O2 = 1.259(5), C2−C1−C6 = 112.8(4), C3−C4−C5 = 112.6(4).

Further, the quinone ligand acquires a boat-like conformation with the quinoid carbons bent out of the diene plane by about 12°, which is smaller than the angle reported for the iridium congener (16°).[9]

While η^4-duroquinone complexes are well-known, [13] we note in contrast that X-ray structures of metal η^4-*p*-quinone compounds are rare; for instance, Stone and co-workers reported the structure of the substituted η^4-quinone platinum complex [(COD)Pt(η^4-$C_6H_2O_2$(Bu^t_2-2,6))].[14] Furthermore, the structure of the anionic manganese *o*-quinone complex [Mn(CO)$_3$(η^4-*o*-benzoquinone)][Na] has been described.[7] Having prepared these compounds, we then decided to investigate their electrochemical behavior in solution.

Electochemistry of Rhodium and Iridium *p*-Benzoquinone Complexes 2a,b. Quinone/hydroquinone redox couples have been widely used in electrochemical studies because they are readily available and exhibit "well behaved" electrochemistry.[4] However, their related metal complexes have attracted less attention.[15a]

(13) (a) Sternberg, H.; Markby, R.; Wender, I. *J. Am. Chem. Soc.* **1958**, *80*, 1009. (b) Fairhurst, G.; White, C. *J. Organomet. Chem.* **1978**, *25*, 243. (c) Fairhurst, G.; White, C. *J. Chem. Soc., Dalton Trans.* **1979**, 1531.

(14) Chetcuti, M. J.; Howard, J. A. K.; Pfeffer, M.; Spenser, J. L.; Stone, F. G. A. *J. Chem. Soc., Dalton Trans.* **1981**, 276.

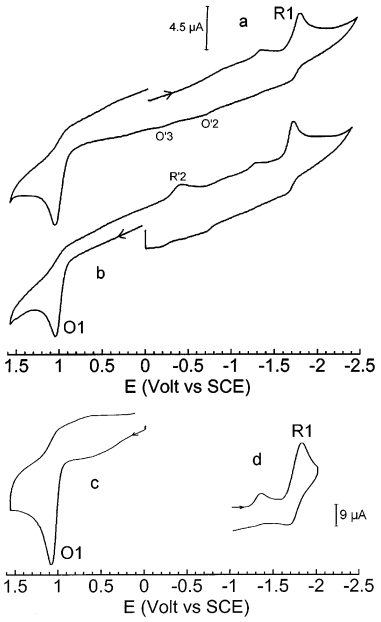

Figure 5. Cyclic voltammetry of the Rh^I complex **2a** (2 mM) in acetonitrile containing n-Bu_4NBF_4 (0.3 M) at a stationary gold-disk electrode (diameter 0.5 mm). With a scan rate of 0.5 V s^{-1}: (a) reduction first; (b) oxidation first. With a scan rate of 20 V s^{-1}: (c) oxidation first; (d) reduction first.

We note, however, that recently Adams and co-workers reported[15b] the electrochemical behavior of a bimetallic carbonyl derivative of 1,4-quinone. In this compound the bonding (μ-η^1:η^1) and the nature of the compound differ completely from those of our π-bonded organometallic quinone complexes. Therefore, to the best of our knowledge this is the first electrochemical study performed on the η^4-π-metalated *p*-benzoquinone complexes **2a**,**b**.

The cyclic voltammetry was performed at room temperature, on a solution of **2a**,**b** (2 mM) in dry and degassed acetonitrile, containing n-Bu_4NBF_4 (0.3 M) as the supporting electrolyte. At a stationary gold-disk electrode (d = 0.5 mm) with a scan rate of 0.5 V s^{-1}, the Rh^I complex **2a** exhibited a reduction peak R_1 at $E^{p}_{R1} = -1.73$ V vs SCE, which was partly reversible (Figure 5a), and an irreversible oxidation peak O_1 at $E^{p}_{O1} = +1.04$ V vs SCE (Figure 5b).

The oxidation peak current of O_1 was ca. twice that of the reduction current of R_1. At higher scan rate (20 V s^{-1}), the peak R_1 became more reversible (Figure 5d), indicating the transfer of one electron. The oxidation peak O_1 was still irreversible (Figure 5c), with a current peak twice that of R_1, attesting to the transfer of two electrons at the potential of O_1. At the scan rate of 0.5 V s^{-1}, we can then assume that the oxidation of **2a** involves two electrons at the potential of O_1, whereas the reduction of **2a** involves one electron (or slightly more than one electron if an ECE mechanism process is involved).[16]

(15) (a) Hiramatsu, M.; Nakano, H.; Fujinami, T.; Sakai, S. *J. Organomet. Chem.* **1982**, *236*, 131. (b) Adams, R. D.; Miao, S. *J. Am. Chem. Soc.* **2004**, *126*, 5056.

(16) The reduction involves one electron for an EC process. If a second electron transfer is involved in an ECE process, at a potential less negative than that of the first electron transfer, then the process involves a second electron transfer at R_1. In the present case, the number of electrons would be slightly higher than 1, since the peak R_1 was partially reversible at low scan rates.

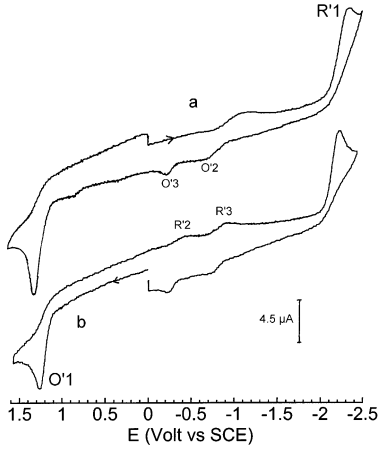

Figure 6. Cyclic voltammetry of the Ir^I complex **2b** (2 mM) in acetonitrile containing n-Bu_4NBF_4 (0.3 M) at a stationary gold-disk electrode (diameter 0.5 mm) with a scan rate of 0.5 V s^{-1}: (a) reduction first; (b) oxidation first.

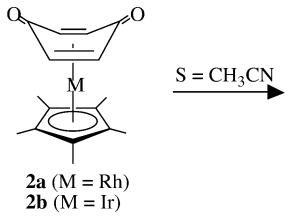

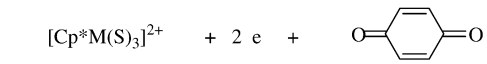

Figure 7. Oxidation of the Rh^I complex **2a** and the Ir^I complex **2b.**

At a stationary gold-disk electrode (d = 0.5 mm) with a scan rate of 0.5 V s^{-1}, the Ir^I complex **2b** exhibited an irreversible reduction peak R'_1 at $E^{p}_{R'1} = -2.23$ V vs SCE (Figure 6a) and an irreversible oxidation peak O'_1 at $E^{p}_{O'1} = +1.26$ V vs SCE (Figure 6b).

Both peaks were irreversible with similar peak currents. They remained irreversible for scan rates up to 200 V s^{-1}. Consequently, we can assume, by comparison with the electrochemical behavior of complex **2a**, that the oxidation and reduction of **2b** is an overall two-electron transfer at the potentials of O'_1 and R'_1, respectively.

Electrochemical Oxidation of 2a,b. After the oxidation of **2b** at O'_1, one observes on the reverse scan two tiny reduction peaks at −0.42 V (R'_2) and −0.89 V (R'_3) (Figure 6b), which characterize the reduction of the species generated in the oxidation of **2b** at O'_1. To identify the reduction process occurring at R'_2 and R'_3, cyclic voltammetry of the benzoquinone was performed under similar conditions. One reversible reduction peak was observed at −0.47 V/−0.40 V (quinone + 1e → [quinone]$^{\bullet-}$), followed by a quasi-reversible process at −1.44 V/−1.40 V vs SCE ([quinone]$^{\bullet-}$ + 1e → [hydroquinone]$^{2-}$).[4] When the oxidation of **2b** was performed in the presence of a small amount of benzoquinone, the reduction peak current at −0.42 V (R'_2) increased on the reverse scan, confirming that the benzoquinone was indeed released in the overall two-electron oxidation of complex **2b**. The oxidation of complex **2b** results then in the oxidation of the Ir^I center to Ir^{III} with release of the free benzoquinone (Figure 7). Since the oxidation peak could not be made reversible, the intimate mechanism of the overall oxidation is not available. One can only assume

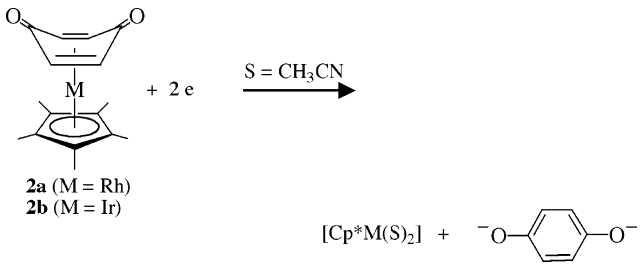

Figure 8. Reduction of the Rh^I complex **2a** and the Ir^I complex **2b**.

that the first electron loss generates the complex $[\mathbf{2b}]^{\bullet+}$, which, after fast decoordination of the quinone, gives a cationic Ir^{II} complex that is more easily oxidized than complex **2b**.

Since an Ir^{III} complex must be released in the two-electron oxidation of complex **2b** (Figure 7), the cyclic voltammetry of $[Cp^*Ir(CH_3CN)_3][OTf]_2$ [10a] (2 mM) in acetonitrile was also performed. It was reduced with an irreversible peak at −1.13 V: i.e., at a potential which was too far from +1.26 V (at which it is generated by the oxidation of **2b**) to be detected, due to the diffusion process at the electrode.

The mechanism of the oxidation of the Rh^I complex **2a**, which involves two electrons at O_1, is then similar to that of the Ir^I complex **2b** (Figure 7). On the reverse scan (Figure 5b) a reduction peak was observed at −0.41 V (R'_2) and assigned to the reduction of the benzoquinone released in the oxidation process. However, one notes that the second reduction peak of the benzoquinone was not detected. An authentic sample of the complex $[Cp^*Rh(CH_3CN)_3][OTf]_2$ [10a] (2 mM) in acetonitrile was reduced in a quasi-reversible peak at −0.53 V/−0.40 V. It should then be detected on the reverse scan just after the reduction peak of the released quinone, except if a fast reaction took place in the diffusion layer, between the radical anion $[quinone]^{\bullet-}$ generated at R'_2 and $[Cp^*Rh(CH_3CN)_3]^{2+}$.[10a] The absence of the second reduction peak of the released benzoquinone is indicative of such a reaction.

Electrochemical Reduction of 2a,b. After the overall two-electron reduction of the Ir^I complex **2b** at R'_1, one observes on the reverse scan two tiny oxidation peaks at $O'_2 = -0.66$ V and $O'_3 = -0.34$ V (Figure 6a), which characterize the oxidation of the species generated in the reduction of **2b** at R'_1. The same oxidation peaks were detected on the reversible scan after reduction of the Rh^I complex **2a** at R_1 (Figure 6a), but at trace levels because of the partial reversibility of the reduction peak R_1. This suggests that a common species was generated by the reduction of **2a** or **2b**: i.e., the dianion $[hydroquinone]^{2-}$ (Figure 8).

A one-electron process was found for complex **2a** at a higher scan rate. We may assume that, in these 18-electron complexes **2a**,**b**, the first electron transfer generates the radical anion $[\mathbf{2a}]^{\bullet-}$ or $[\mathbf{2b}]^{\bullet-}$ with the electron located on the ligand (Figure 9); $[\mathbf{2a}]^{\bullet-}$ is more stable than $[\mathbf{2b}]^{\bullet-}$ within the time scale of the cyclic voltammetry investigated here. The radical anion $[\mathbf{2b}]^{\bullet-}$ undergoes a fast rearrangement which results in the reorganization of the reduced ligand to generate the new complex $[Cp^*Ir(\eta^4\text{-benzoquinone})]^{\bullet-}$ (Figure 9). The subsequent evolution of the latter complex, by either route A or route B, is speculative. Indeed, the second electron transfer may occur either on the $[quinone]^{\bullet-}$ ligand in the intermediate complex (route A), which would be more easily reduced than **2b**, or on the free $[quinone]^{\bullet-}$ (route B), which is immediately reduced to $[hydroquinone]^{2-}$ at the potential of R'_1. This explains the transfer of two electrons at the potential of R'_1.

As far as the Rh complex **2a** is concerned, the mechanism of its reduction is the same, except that the complex $[\mathbf{2a}]^{\bullet-}$ generated in the first electron transfer is more stable than $[\mathbf{2b}]^{\bullet-}$, indicated by the partial reversibility of its reduction peak. As a consequence, the two successive oxidation peaks O'_2 and O'_3 of the released dianionic $[hydroquinone]^{2-}$ were present at trace levels on the reverse scan (Figure 5a).

Concluding Remarks

In conclusion we report the high-yield synthesis of the π-bonded semiquinone complexes $\{[Cp^*M(\eta^5\text{-semiquinone})][OTf]\}_n$ (M = Rh (**1a**), M = Ir (**1b**)). The latter complexes exhibit a hydrogen-bonding interaction in

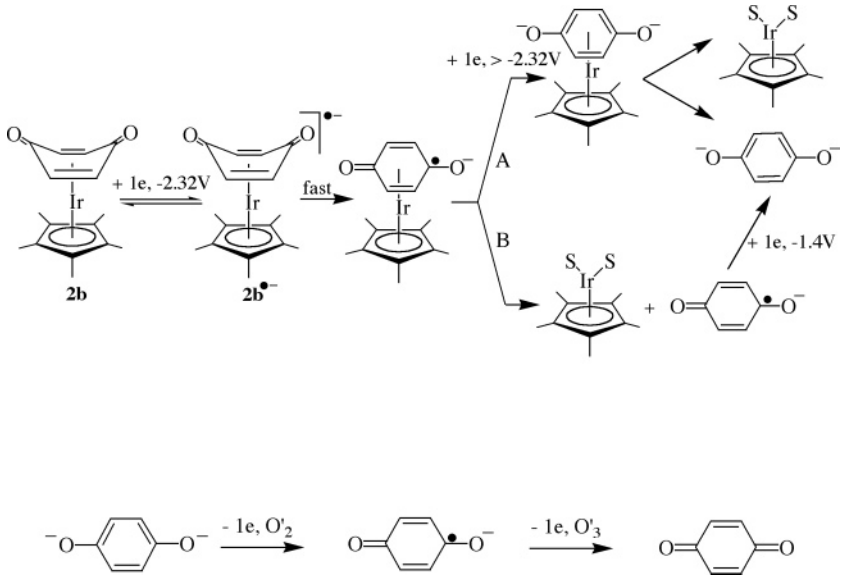

Figure 9. Proposed mechanism for the reduction of **2b**.

solution, as indicated by their NMR spectra. X-ray structures of **1a**,**b** support these findings and show the formation of organometallic polymers where the integrity of the system is maintained by strong hydrogen bonding (O- - -O, d = 2.45 Å) between π-metalated semiquinone subunits. Deprotonation of **1a** provides the related η^4-quinone complex [Cp*Rh(η^4-quinone)] (**2a**) completely characterized, including its X-ray structure. The electrochemistry of these π-bonded quinone complexes [Cp*M(η^4-quinone)] (M = Rh (**2a**), M = Ir (**2b**)) carried out for the first time provide us with valuable information concerning their behavior relative to the free quinone ligand, an important species in chemistry and biology. Thus, the electrochemical oxidation of complexes **2a**,**b** is an overall two-electron uptake, which results in the oxidation of the metal(I) center to a metal(III) complex with release of the free quinone. The electroreduction of both complexes affects the η^4 ligand. It proceeds in one overall two-electron step for the Ir^I complex **2b**, leading to the dianionic [hydroquinone]$^{2-}$, whereas the 19-electron intermediate Rh^I complex [**2a**]$^{\bullet-}$ generated after the first electron transfer on the Rh^I complex **2a** was more stable. As a result, the oxidation process generates the free quinone, whereas the reduction process generates the reduced form of the quinone. It is worthwhile to note that the η^4-ligated benzoquinone was reduced in both complexes **2a**,**b**, at much more negative potentials than for the free benzoquinone, which is in agreement with the nonconjugated character of the carbonyl groups in the η^4 complexation mode. It also indicates that π-metalated benzoquinone complexes **2a**,**b** are more stable than the free benzoquinone.

Experimental Section

General Considerations. All manipulations were carried out under an argon atmosphere using Schlenk techniques. Solvents were purified and dried prior to use by conventional distillation techniques. Acetone was distilled over K_2CO_3, diethyl ether was distilled over Na, and CH_2Cl_2 was distilled over CaH_2. All reagents obtained from commercial sources were used without further purification. ^{1}H NMR spectra were recorded on Bruker AM 300 MHz and Avance 400 MHz instruments. ^{1}H NMR chemical shifts are reported in parts per million referenced to a residual solvent proton resonance.

General Procedure for Cyclic Voltammetry. Cyclic voltammetry was performed in a three-electrode cell connected to a Schlenk line, at room temperature. The counter electrode was a platinum wire of ca. 1 cm^2 apparent surface area. The reference was a saturated calomel electrode (Radiometer Analytical) separated from the solution by a bridge filled with 3 mL of acetonitrile containing nBu$_4$NBF$_4$ (0.3 M). The working electrode was a stationary gold disk (0.5 mm diameter). Complex **2a** (10.4 mg, 0.03 mmol) was introduced into 15 mL of acetonitrile containing nBu$_4$NBF$_4$ (0.3 M), and the cyclic voltammetry was performed at various scan rates. The same experiments were carried out with complex **2b** (14.1 mg, 0.03 mmol).

Synthesis of {[Cp*Rh(η^5-semiquinone)][CF_3SO_3]}$_n$ (1a). A solution of $AgCF_3SO_3$ (175 mg, 0.68 mmol) in acetone (10 mL) was added to [(η^5-C_5Me_5)Rh(μ-Cl)Cl]$_2$ (100 mg, 0.17 mmol) in acetone (15 mL), to rapidly give a white precipitate of AgCl. The reaction mixture was stirred for 10 min, and then the resulting orange solution of [(η^5-C_5Me_5)Rh(acetone)$_3$][CF_3SO_3]$_2$ was filtered into a dry Schlenk tube kept under argon. To this orange solution was then added hydroquinone (112 mg, 1.0 mmol) in acetone (10 mL). The solution immediately became yellow, and the mixture was stirred for 15 min; then the solvent was removed under vacuum and the volume was reduced. Subsequent addition of Et_2O (20 mL) afforded a yellow precipitate. This compound was separated and washed several times with Et_2O and dried under vacuum, leaving **1a** (158 mg, 95%,). Mp: 195 °C dec. Spectroscopic data for **1a** are as follows. IR (KBr disk, cm^{-1}): ν(C=O) 1500, ν($CF_3SO_3^-$) 1234, 1024, ν(−OH) 3361. ^{1}H NMR (CD_3OD, 400 MHz): δ 2.09 (s, 15H, η^5-C_5Me_5), 6.13 (s, 4H dienyl CH), 6.61 (s, 1H, OH). ^{13}C{^{1}H} NMR (100.62 MHz, CD_3OD): δ 145.39 (s, C=O), 116.79 (s, C−OH), 108.09 (d, J_{Rh-C} = 7.6 Hz, $C_5(CH_3)_5$, −C=C−), 92.27(d, J_{Rh-C} = 6 Hz, −C=C−, semiquinone), 9.68 (s, $C_5(CH_3)_5$, $-CH_3$). Anal. Calcd for $C_{17}H_{20}O_5F_3SRh\cdot 2CH_2Cl_2$: C, 34.26; H, 3.63. Found: C, 34.12; H, 3.62.

Synthesis of {[Cp*Ir(η^5-semiquinone)][CF_3SO_3]}$_n$ (1b). This compound was prepared in a way similar to that for **1a** and was obtained as a white microcrystalline substance in 94% yield (137 mg). Mp: 180 °C dec. Spectroscopic data for **1b** are as follows. IR (KBr disk, cm^{-1}): ν(C=O) 1503, ν($CF_3SO_3^-$) 1234, 1029, ν(−OH) 3400. ^{1}H NMR (CD_3OD, 400 MHz): δ 2.19 (s, 15H, η^5-C_5Me_5), 6.03 (s, 4H dienyl CH), 6.61 (s, 1H, OH). ^{13}C{^{1}H} NMR (100.62 MHz, CD_3OD): δ 145.31 (s, C=O), 116.79 (s, C−OH), 101.39 (s, $C_5(CH_3)_5$, −C=C−), 81.60 (s, −C=C−, semiquinone), 9.41 (s, $C_5(CH_3)_5$, $-CH_3$). Anal. Calcd for $C_{17}H_{20}O_5F_3SIr\cdot 2CH_2Cl_2$: C, 30.21; H, 3.20. Found: C, 30.55; H, 3.24.

Synthesis of [Cp*Rh(η^4-benzoquinone)] (2a). A suspension of t-BuOK (144 mg, 1.2 mmol) in CH_2Cl_2 (10 mL) was added to a suspension of {[Cp*Rh(η^5-semiquinone)][CF_3SO_3]}$_n$ (**1a**; 200 mg, 0.4 mmol) in CH_2Cl_2 (10 mL). The mixture was left for 3 h, during which time the solution became yellow-orange. The mixture was filtered to give a bright yellow-orange solution. The solvent was removed under vacuum, and the yellow microcrystalline material was dried (95 mg, 65%). Mp: 280 °C dec. Spectroscopic data for **2a** are as follows. IR (KBr disk, cm^{-1}): ν(C=O) 1535, 1565. ^{1}H NMR (CD_3CN, 400 MHz): δ 1.92 (s, 15H, η^5-C_5Me_5), 4.82 (s, 4H dienyl C−H). ^{13}C-{^{1}H} NMR (100.62 MHz, CD_3CN): δ 157.39 (s, C=O), 101.78 (d, J_{Rh-C} = 7 Hz, $C_5(CH_3)_5$, −C=C−), 86.59 (d, J_{Rh-C} = 7.5 Hz, −C=C−, benzoquinone), 9.81 (s, $C_5(CH_3)_5$, $-CH_3$). Anal. Calcd for $C_{16}H_{19}O_2Rh\cdot 2H_2O$: C, 50.27; H, 6.06. Found: C, 49.66; H, 6.30.

X-ray Crystal Structure Determination for 1a,b and 2a. Suitable crystals of {[Cp*Rh(η^5-semiquinone)][CF_3SO_3]}$_n$ (**1a**) and {[Cp*Ir(η^5-semiquinone)][CF_3SO_3]}$_n$ (**1b**) were obtained using slow-diffusion techniques from MeOH/ether solution, while those of [Cp*Rh(η^4-benzoquinone)] (**2a**) were obtained at room temperature by slow diffusion of ether into a saturated solution of **2a** in CH_2Cl_2. The selected crystals of complexes **1a**,**b** and **2a** were protected by Paratone oil and Araldite and then mounted on the top of a glass rod. The data were collected at room temperature on a Nonius KappaCCD diffractometer with graphite-monochromated Mo Kα radiation. The Nonius Supergui program package was used for cell refinement and data collection. The structure was solved by direct methods and subsequent difference Fourier treatment and refined by full-matrix least squares on F using the programs of the PC version of CRYSTALS.[17] All non-solvent molecules and non-hydrogen atoms were refined anisotropically. In **1a**, one of the triflate anions was refined isotropically, and in **1b** both anions were refined isotropically, while in **2a** all atoms were refined anisotropically. Hydrogen atoms were introduced in calculated positions in the last refinements and were allocated overall refinable isotropic thermal parameters. Fractional parameters, anisotropic thermal parameters, and

(17) Watkin, D. J.; Prout, C. K.; Carruthers, R. J.; Betteridge, P. W. CRYSTALS Issue 10; Chemical Crystallography Laboratory, Oxford, U.K., 1996.

all bond lengths and angles are given in the Supporting Information for complexes **1a**,**b** and **2a**.

Acknowledgment. We would like to thank the CNRS, the "Université Pierre et Marie Curie", and the Ecole Normale Supérieure for supporting this work.

Supporting Information Available: X-ray crystallographic files in CIF format for the structure determinations of **1a**,**b** and **2a**. This material is available free of charge via the Internet at http://pubs.acs.org.

OM049292T